Endocannabinoid signaling modulates neurons of the pedunculopontine nucleus (PPN) via astrocytes

Endocannabinoid signaling in the PPN

Áron Kőszeghy[1*]; Adrienn Kovács[1*]; Tamás Bíró[1,2]; Péter Szücs[1,5], János Vincze[1], Zoltán Hegyi[3], Miklós Antal[3,4], Balázs Pál[1**]

[1]Department of Physiology, Faculty of Medicine, University of Debrecen, Debrecen, Hungary

[2]„DE-MTA Lendület" Cellular Physiology Research Group of the Hungarian Academy of Sciences

[3]Department of Anatomy, Histology and Embryology; Faculty of Medicine, University of Debrecen, Debrecen, Hungary

[4]MTA-DE Neuroscience Research Group, Faculty of Medicine, University of Debrecen, Debrecen, Hungary

[5]MTA-DE-NAP B- Pain Control Research Group, Faculty of Medicine, University of Debrecen, Debrecen, Hungary

[*]These authors contributed equally to this work.

[**]Corresponding author: Balázs Pál MD, PhD

Department of Physiology, Faculty of Medicine, University of Debrecen,

4012 Debrecen, Nagyerdei krt 98.

e-mail: pal.balazs@med.unideb.hu

Phone: +36-52-255-575

Fax: +36-52-255-116

Abstract

The pedunculopontine nucleus (PPN) is known as the cholinergic part of the reticular activating system (RAS) and it plays an important role in transitions of slow wave sleep to REM sleep and wakefulness. Although both exogenous and endocannabinoids affect sleep, the mechanism of endocannabinoid neuromodulation has not been characterized at cellular level in the PPN.

In this paper we demonstrate that both neurons and glial cells from the PPN respond to cannabinoid type 1 (CB1) receptor agonists. The neuronal response can be depolarization or hyperpolarization, while astrocytes exhibit more frequent calcium waves. All of these effects are absent in CB1 gene deficient mice. Blockade of the fast synaptic neurotransmission or neuronal action potential firing does not change the effect on the neuronal membrane potential significantly, while inhibition of astrocytic calcium waves by thapsigargin diminishes the response. Inhibition of group I metabotropic glutamate receptors (mGluRs) abolishes hyperpolarization, whereas blockade of group II mGluRs prevents depolarization. Initially active neurons and glial cells display weaker responses partially due to the increased endocannabinoid tone in their environment.

Taken together, we propose that cannabinoid receptor stimulation modulates PPN neuronal activity in the following manner: active neurons may elicit calcium waves in astrocytes via endogenous CB1 receptor agonists. Astrocytes in turn release glutamate, that activates different metabotropic glutamate receptors of neurons and modulate PPN neuronal activity.

Keywords

Introduction

The pedunculopontine nucleus (PPN) is thought to play an important role in the transitions of slow wave sleep (SWS) either to wakefulness or to rapid eye movement (REM) sleep, as increased activity of this nucleus was observed in wakefulness and REM sleep (Garcia-Rill, 1991, 2011; Reese et al., 1995; Winn, 2006). The PPN is a part of the reticular activating system and is known as one of the main sources of the cholinergic fibers (Maloney et al., 1999; Jenkinson et al., 2009).

Besides the cholinergic neurons, the PPN is also composed of non-cholinergic cells, which are mostly GABAergic and glutamatergic. Several cholinergic and GABAergic neurons of the nucleus show synchronicity with the slow wave cortical activity: the majority of the cholinergic neurons fire synchronously with the 'up' state, known as the active component; whereas certain non-cholinergic cells are active during the 'down' state. Parallel with the cortical gamma-activity, most of the cholinergic cells increase their firing rate, while non-cholinergic cells increase, decrease or do not change their firing rate (Mena-Segovia et al., 2008, Ros et al., 2010).

Endocannabinoids have multiple effects on brain functions via modulating several signaling processes and synaptic connections (Katona and Freund, 2012). Among several other effects, CB1 receptor stimulation is able to modify the sleep-wake cycles. Early studies indicated that REM sleep duration and the eye movement activity is affected in marijuana smokers (Feinberg et al., 1975). In vivo animal experiments revealed that the prototypic endocannabinoid anandamide injected intracerebroventricularly or directly to the PPN reduced wakefulness and increased both SWS and REM sleep. As CB1 receptor

antagonists are able to reverse the effect of anandamide on sleep, it was hypothesized that the sleep modulation of the endocannabinoids is taking place via CB1 receptors (Murillo-Rodriguez, 2008; Murillo-Rodriguez et al., 2008; Herrera-Solís et al., 2010).

Besides the well described presynaptic inhibition of neurotransmitter release by activation of CB1 receptor (Katona et al., 1999; Wilson and Nicoll, 2001; Kawamura et al., 2006), there is a growing body of evidence suggesting that astrocytes also possess CB1 receptors and have a role in endocannabinoid signaling. Astrocytic CB1 receptors were shown in the cerebellum and the spinal cord (Hegyi et al., 2009, 2012; Rodriguez-Cueto et al., 2013). Furthermore, it was recently demonstrated that hippocampal astrocytes are directly activated by cannabinoid receptor agonists and modify synaptic neurotransmission by releasing gliotransmitters, i.e. glutamate (Navarrete and Araque, 2008, 2010; Han et al., 2012; Min and Nevian, 2012; Coiret et al., 2012).

Despite of its potential importance, to our knowledge, no data exist about the cellular actions of exogenous or endocannabinoids in the PPN. In this work, the effects of CB1 receptor agonists on the cells of the PPN were investigated. We showed that neurons of the PPN respond in a heterogeneous way to CB1 receptor stimulation. This response is due to the direct activation of astrocytes and their consequential glutamate release, which can either depolarize or hyperpolarize PPN neurons via different metabotropic glutamate receptors.

Materials and methods

Solutions, chemicals

Experiments were performed in an artificial cerebrospinal fluid (aCSF) of the following composition (in mM): NaCl, 120; KCl, 2.5; NaHCO3, 26; glucose, 10; NaH2PO4, 1.25; CaCl2, 2; MgCl2, 1; myo-inositol, 3; ascorbic acid, 0.5; and sodium-pyruvate, 2; pH 7.2. For the slice preparation a modified aCSF (low Na aCSF) was used where 95 mM NaCl was replaced by sucrose (130 mM) and glycerol (60 mM). All chemicals were purchased from Sigma (St. Louis, MO, USA), unless stated otherwise.

Animals, preparation

Animal experiments were conducted in accordance with the appropriate international and Hungarian laws and institutional guidelines on the care of research animals. The experimental protocols were approved by the Committee of Animal Research of the University of Debrecen. 8-15 days old C3H mice (n = 58), as well as mice expressing tdTomato fluorescent proteins in a GAD2- (n = 12) or ChAT-dependent way (n = 17) were used from both sexes. The floxed-stop-tdTomato (Madisen et al., 2010; JAX mice accession number 007905), GAD2-cre (Taniguchi et al., 2011; JAX number: 010802) and ChAT-cre (Lowell et al., 2006; http://www.informatics.jax.org/reference/J:114556; JAX number: 006410) mouse lines were purchased from Jackson Laboratories (Bar Harbor, ME, USA) and crossed in the

animal house of the Department of Physiology. In some cases, CB1 receptor knockout mice (n = 9; a kind gift from A. Zimmer - Bonn, Germany) and wild type littermates (n = 5) were also used (Zimmer et al., 1999).

After decapitation of the animal and removal of the brain, 200 μm-thick coronal midbrain slices were prepared in ice-cold low Na aCSF using a Microm HM 650V vibratome (Microm International GmbH, Walldorf, Germany). The slices were incubated in normal aCSF for 60 minutes on 37°C.

Electrophysiology

Brain slices were visualized with a Zeiss Axioskop microscope (Carl Zeiss AG, Oberkochen, Germany). Patch pipettes with 5 MΩ pipette resistance were fabricated, and filled with a solution containing (in mM): K-gluconate, 120; NaCl, 5; 4-(2-hydroxyethyl)-1- piperazineethanesulfonic acid (HEPES), 10; EGTA, 2; $CaCl_2$, 0.1; Mg-ATP, 5; Na3-GTP, 0.3; Na2- phosphocreatinine, 10; biocytin, 8; pH 7.3. Whole-cell patch-clamp recordings were performed using an Axopatch 200A amplifier (Molecular Devices, Union City, CA, USA). All recordings were performed on room temperature. Data acquisition was achieved using the Clampex 10.0 software (Molecular Devices, Union City, CA, USA), while data analysis was performed using the Clampfit 10.0 (Molecular Devices) or MiniAnalysis (Synaptosoft, Decatur, GA, USA) programs.

Membrane potential measurements

For comparing the membrane potentials two 120-second-long trace segments were selected: one from the control period and another starting at 3 minutes after the beginning of drug administration. Histograms of the membrane potential values were constructed from these periods and the value corresponding to the largest bin was considered as resting membrane potential. In those experiments where membrane potential changes were monitored continuously to demonstrate the time-course of the drug effect, the above mentioned procedure was performed at every 30 seconds of the trace.

As the resting membrane potential of spontaneously firing neurons could not be measured, a median voltage that corresponded to the baseline potential was determined from the membrane potential histograms of these neurons. (Suppl. Fig. 1)

Pharmacology

To activate CB1 receptors, arachidonyl–2'–chloroethylamide (ACEA) was administered at a concentration of 5 μM, whereas WIN55,212-2 was used in 1 μM. The anandamide membrane transport inhibitor, UCM707, was applied in 10 μM concentration. In certain experiments, slices were continuously perfused with 10 μM 2,3–dihydroxy–6–nitro–7–sulfamoyl-benzo[f]quinoxaline–2,3–dione (NBQX), 50 μM D–2–amino–5–phosphonopentanoate (D-AP5; Tocris Cookson Ltd., Bristol, UK), 1 μM strychnine, and 10 μM bicuculline in order to block ionotropic glutamatergic, glycinergic and GABAergic neurotransmissions. In further experiments, 100 μM 7–(Hydroxyimino)cyclopropa[b]chrome–n–1a–carboxylate ethyl ester (CPCCOEt) and 10

µM 2–Methyl–6– (phenylethynyl)pyridine hydrochloride (MPEP) were used to block type 1 and 5 metabotropic glutamate receptors (group I mGluRs), respectively; while 10 µM LY341495 was added to block group II mGluRs. Spontaneous action potential firing was blocked by 1 µM tetrodotoxin (TTX). In other experiments, slices were preincubated with 50 nM ACEA for 5-7 minutes, before the application of 5 µM ACEA.

Calcium imaging

Details of the calcium imaging were described by Kőszeghy et al. (2012). Briefly, for calcium imaging the acetoxymethylester form of the Oregon Green 488 BAPTA 1 fluorescent dye (OGB; Invitrogen-Molecular Probes, Carlsbad, CA, USA) was used. Slices were incubated with 33 µM OGB for 25 min (37°C, 95% O_2, 5% CO_2) in order to load the cells with the dye.

The slices were visualized with a Zeiss Axioskop microscope (Carl Zeiss AG). The microscope was equipped with a fluorescent imaging system (Till Photonics GmbH, Gräfeling, Germany) containing a xenon bulb-based Polychrome V light source, a CCD camera (SensiCam, PCO AG, Kelheim, Germany), an imaging control unit (ICU), and the Till Vision software (version 4.0.1.3). The excitation wavelength was set to 488 nm. The fluorescent filter set was composed of a dichroic mirror (Omega XF2031 505DRLPXR; Omega Drive, Brattleboro, VT, USA) and an emission filter (LP 515, Till Photonics). Throughout the calcium imaging, frames with 344 x 260 pixel resolution were employed with a frame rate of 10 Hz. In parallel with the imaging, patch-clamp experiments were also performed.

In order to confirm glial origin of the slow calcium waves, whole-cell patch-clamp recordings were performed on cells displaying slow calcium waves. These cells were filled with Alexa Fluor 594 (Invitrogen-Molecular Probes) for the morphological identification (n = 4). Furthermore, loose-patch recordings on cells with slow calcium waves were also performed in some cases (n = 8, data not shown) in order to verify the absence of action potentials.

In certain experiments, slices were incubated with 1 μM thapsigargin for 45 minutes to inhibit astrocytic calcium waves in the slices.

Visualization of the labeled neurons

The neurons were filled with biocytin during the electrophysiological recordings. The slices accommodating the filled neurons were fixed overnight (4% paraformaldehyde in 0.1M phosphate buffer; *pH* 7.4; 4 °C). Permeabilization was achieved in Tris buffered saline (in mM, Tris base, 8; Trisma HCl, 42; NaCl, 150; *pH* 7.4) supplemented with 0.1% Triton X-100 and 10% bovine serum (60 min). The slices were incubated in phosphate buffer containing streptavidin-conjugated Alexa488 (1:300; Molecular Probes Inc., Eugene, OR, USA) for 90 min. In samples with no tdTomato expression, *post hoc* ChAT-immunohistochemistry was performed following the biocytin recovery (goat anti-ChAT diluted 1:500; Millipore, Temecula, CA; and Texas Red rabbit-anti-goat secondary antibody diluted in 1:1000; Vector Laboratories Inc., Burlingame, CA, USA). The cells were visualized using a Zeiss LSM 510 confocal microscope (Carl Zeiss AG).

Immunohistochemistry

Experiments were carried out on 3 mice expressing tdTomato in ChAT-dependent manner and additionally on 3 wild type C3H mice. Animals were deeply anesthetized with sodium pentobarbital (50 mg/kg, i.p.) and transcardially perfused with Tyrode's solution (oxygenated with a mixture of 95% O_2, 5% CO_2), followed by a fixative containing 4% paraformaldehyde dissolved in 0.1 M phosphate buffer (PB, pH 7.4). After the transcardial fixation, the mesencephalon was removed, postfixed in the original fixative for 4 hours, and immersed into 10% and 20% sucrose dissolved in 0.1 M PB until they sank. In order to enhance reagent penetration the removed mesencephalons were freeze-thawed. Fifty-micrometer thick transverse sections were cut on a vibratome, and the sections were extensively washed in 0.1 M PB.

A single immunostaining protocol was performed to study the cellular distribution of CB1-R in the PPN. Free-floating sections were first incubated in rabbit anti-CB1 receptor antibody (diluted 1:5000; Cayman Chemical, Ann Arbor, MI) for 48 h at 4 °C, and then were transferred into anti-rabbit IgG conjugated with Alexa Fluor 647 (diluted 1:1,000; Invitrogen, Eugene, OR). Before the antibody treatments the sections were kept in 10% normal goat serum (Vector Labs., Burlingame, California, USA) for 50 min. Antibodies were diluted in 10 mM TPBS (pH 7.4) containing 1% normal goat serum (Vector Labs., Burlingame, CA). Sections were mounted on glass slides and covered with Vectashield (Vector Labs, Burlingame, CA).

Double-immunostaining protocols were performed to study the co-localization of CB1-R immunoreactivity with glial fibrillary acidic protein (GFAP), a marker of astrocytes. Free-floating sections were first incubated with a mixture of antibodies that contained rabbit anti-CB1 receptor (diluted 1:2000, Cayman Chemical, Ann Arbor, MI), mouse anti-GFAP (diluted 1:1,000; Millipore, Temecula, CA). The sections were incubated in the primary antibody solutions for 2 days at 4 °C and were transferred for an overnight treatment into the appropriate mixtures of secondary antibodies that contained goat anti-rabbit IgG conjugated with Alexa Fluor 647 (diluted 1:1000; Invitrogen, Eugene, OR) and goat anti-mouse IgG conjugated with Alexa Fluor 488 (diluted 1:1000; Invitrogen, Eugene, OR). Before the antibody treatments the sections were kept in 10% normal goat serum (Vector Labs., Burlingame, CA) for 50 min. Antibodies were diluted in PBS (pH 7.4) containing 1% normal goat serum (Vector Labs., Burlingame, CA). Sections were mounted on glass slides and covered with Vectashield (Vector Labs, Burlingame, CA).

Series of 1 μm thick optical sections with 500 nm separation in the z-axis were scanned with an Olympus FV1000 confocal microscope. Scanning was carried out using a 60x PlanApo N oil-immersion objective (NA: 1.42) and FV10-ASW software (Olympus). The scanned images were processed with Adobe Photoshop CS6 software. Confocal settings including confocal aperture, laser power, gain, offset and pixel size were identical for all scans. By filtering the background staining out with a high-pass intensity filter, threshold values were set for both CB1-R and the other markers.

The specificity of the primary antibody against CB1 receptor (Cayman Chemical, Ann Arbor, MI) has extensively been characterized previously, using knockout control

(Hegyi et al, 2009). To test the specificity of the immunostaining protocol, free-floating sections were incubated according to the immunostaining protocol described above with primary antibodies omitted or replaced with 1% normal goat serum. No immunostaining was observed in these sections.

For quantitative analysis of co-localization of CB1-R- and GFAP-immunopositivity, free-floating sections were first incubated with a mixture of antibodies that contained rabbit anti-CB1-R (1:2000, Cayman Chemical), goat anti-ChAT (1:500, Millipore) and mouse anti-GFAP (1:1000, Millipore). The sections were first incubated in the primary antibody solutions for 2 days at 4 °C, followed by a treatment with an appropriate mixtures of secondary antibodies that were selected from the following: donkey anti-rabbit IgG conjugated with Alexa Fluor 555 (1:1000, Invitrogen), donkey anti-goat IgG conjugated with Alexa Fluor 488 (1:1000, Invitrogen), and donkey anti-mouse IgG conjugated with Alexa Fluor 647 (1:1000, Invitrogen).

The co-localization of CB1 receptor immunoreactive puncta with astrocytic (GFAP-IR) profiles was quantitatively analyzed in the multiple stained sections. A 10x10 standard square grid in which the edge-length of the unit square was 5 µm (the whole grid was 50 µm x 50 µm in size) was placed onto the regions of confocal images corresponding to the PPN. CB1 receptor immunoreactive profiles over the edges of the standard grid were selected and examined whether they were also immunoreactive for the axonal or glial markers. The quantitative measurement was carried out in three sections that were randomly selected from three animals. Thus, the calculation of quantitative

data, mean values and standard error of means (SEM), was based on the investigation of nine sections.

Statistical analysis

All data are represented as mean ± SEM. To compare the central tendency (mean or median) of two independent datasets, either Student's t-test or the Mann-Whitney U-test was used. For comparisons involving multiple datasets, either ANOVA or Kruskal-Wallis ANOVA on Ranks was performed, followed by an appropriate post hoc test (Tukey's and Dunn's test, respectively) to test for pairwise differences. For the comparison of before and after values, either the paired form of Student's t-test or the Signed Rank Test was used.

Parametric and nonparametric tests were used as appropriate for the given dataset. Generally speaking, changes of the resting membrane potential showed Gaussian distribution and parametric tests were applied, while most other parameters, including the resting membrane potential or the firing frequency of calcium waves and the change of the latter showed non-Gaussian distribution and non-parametric tests were used. In cases where the magnitude of effects caused by the application of a treatment was to be compared, the absolute value of the change in the parameter value was taken. To evaluate the differences in the pattern of resting membrane potential changes among groups, neurons were grouped according to their resting membrane potential changes (depolarized, hyperpolarized and no change, 2 mV cutoff) and Fisher's exact test was used to check the relationship between the treatment groups and the response groups,

used together with Bonferroni correction of the obtained p values when pairwise comparisons were done. A similar approach was used for used for frequency changes with a cutoff of 0.5 Hz. General correlation between datasets was evaluated using Spearman's correlation coefficient (S). For all tests p values below 0.05 were accepted as significant. When Bonferroni correction was applied, the corrected p values are given. Calculations were done using the statistical module SigmaPlot 12 (Systat Software, San Jose, CA) and GraphPad Prism 6 (GraphPad Software, La Jolla, CA).

Results

CB1 receptor activation evokes heterogeneous response in PPN neurons.

Whole-cell patch-clamp recordings were performed in order to characterize the effects of CB1 receptor stimulation on the membrane potential and the firing pattern of the PPN neurons (n=46). The location of the cells was confirmed and their morphological characteristics were revealed with biocytin labeling. All cells were located dorsally from the superior cerebellar peduncle in its vicinity (within 100 μm), and medially from the lateral lemniscus, both from the pars compacta and pars dissipata (Fig.1a-i). In some cases, neurons were identified by tdTomato fluorescent protein expressed in a ChAT- or GAD65-dependent way (Fig.1d-i). The average resting membrane potential of the recorded neurons was -57.4 ± 1.3 mV. However, 54% of the neurons fired action potentials spontaneously, with an average rate of 1.85 ± 0.35 Hz; the baseline potential for these spontaneously active cells were -53.6 ± 1.75 mV (n=25).

Cells responded to 5 μM ACEA in different ways: some depolarized and increased action potential firing frequency; others hyperpolarized, reduced firing frequency or stopped completely (Fig.1j-k, Suppl. Fig. 1). The remaining cells showed minimal or no response. PPN neurons from CB1 receptor deficient mice (n = 13) showed smaller membrane potential alterations when compared to control animals (Fig.1k)

In order to exclude bias originating from spontaneous fluctuations of the neuronal resting membrane potential and firing rate, we analyzed 13 neurons where we had at least 7 minutes recording in naCSF without drug application. In these cases, the membrane potential and firing rate values from the last 2 minutes were compared to the values taken

from the first 2 minutes of these traces. The magnitude of spontaneous resting membrane potential fluctuations proved significantly smaller (1.031 ± 0.183 mV vs 4.322 ± 0.477 mV in control; p<0.001; Suppl. Fig.2a) than changes of the same parameters after 5μM ACEA. Neurons from CB1 knockout mice showed similarly small changes of the resting membrane potential (magnitude of resting membrane potential fluctuations: 0.838 ± 0.243 mV, p<0.0001 vs control, p>0.9999 vs no treatment). In 4 further cases, membrane potential and action potential firing rate were recorded for 10 minutes under control conditions, and the membrane potential and firing rate of the first and last minute of the trace were compared. The average change of the resting membrane potential was 2 ± 0.52 mV, whereas the average change of the firing rate was 0.52 ± 0.19 Hz.

Another cannabinoid receptor agonist, WIN55,212-2 (1 μM; n = 16) and the anandamide membrane transport inhibitor UCM707 (10 μM; n = 13) also elicited a similar effect. No significant differences could be revealed between the effects of the three applied CB1 receptor agonists on the pattern of resting membrane potential (p = 0.7308) or firing frequency changes (p = 0.6611 for multi-group comparison; Suppl. Fig. 2b-c).

In an additional set of neurons, voltage-clamp experiments (n = 28) were also performed in order to confirm the results obtained with current clamp recordings. At -60 mV holding potential, 5 μM ACEA elicited an inward current in 11 cases (-24.5 ± 4.4 pA), outward current in 7 cases (19 ± 1.9 pA) and failed to change the holding current in 10 further cases (data not shown).

This heterogeneity of the observed response can potentially depend on the neuronal type. Therefore, tdTomato expressing cholinergic and GABAergic neurons were patched. Both cell groups exhibited all three types of responses to ACEA application; however, the proportions of the responses were different. Cholinergic cells were depolarized, hyperpolarized or lacked response in similar proportions, whereas the majority of the GABAergic neurons were depolarized (Fig.2a-b). Four out of the 9 neurons identified as cholinergic displayed stronger depolarization than 2 mV, 2 hyperpolarized stronger than 2 mV and membrane potential changes did not exceed 2 mV in 3 further cases. 7 from the 10 non-cholinergic neurons were depolarized and 3 were hyperpolarized.

Blockade of the neuronal activity by 1 μM TTX or inhibition of fast synaptic neurotransmission by a cocktail composed of NBQX (10 μM), D-AP5 (50 μM), strychnine (1 μM) and bicuculline (10 μM) did not change the effects of ACEA on resting membrane potential significantly (Fig.2c-d). The blocking cocktail, however, completely abolished spontaneous (n = 6) and evoked postsynaptic currents (n = 13).

In the next series of experiments slices were preincubated with group I or group II mGluR antagonists; 10 μM MPEP and 100 μM CPCCOEt, or 10 μM LY341495, respectively. Interestingly, after preincubation with group I mGluR blockers neurons were either depolarized or unaffected by ACEA, but only a single case of small amplitude hyperpolarization was observed (Fig.2e).

In contrast to group I mGluR blockers, after the preincubation with the group II mGluR inhibitor LY341495 application of ACEA either caused robust hyperpolarization, no effect or, in a few cases, depolarization with small amplitude (Fig.2f).

Finally, when using blockers of the fast synaptic neurotransmission together with group I and II mGluR antagonists, application of ACEA resulted in no significant change of the resting membrane potential or firing frequency in the recorded neurons (Fig.2g).

Activation of CB1 receptors alters astrocyte calcium wave frequency

Since, blockade of fast synaptic transmission and action potential firing did not abolish the cannabinoid induced neuronal membrane potential changes; we tested whether activation of astrocytes via CB1 receptors may be influencing neuronal activity. Slices were loaded with OGB calcium sensitive dye, and changes of the fluorescence intensity were detected. First we wanted to confirm that in accordance with our previous results in the cochlear nucleus (Kőszeghy et al., 2012), and with the findings of other authors in the cortex (Nimmerjahn et al., 2004.), cells exhibiting slow calcium waves in the PPN are glia. Whenever whole-cell (n = 4) or loose-patch (n = 8; data not shown) recordings were performed from cells producing slow calcium waves action potential discharge was never observed and the characteristic astrocyte morphology was revealed after loading the cells with Alexa 594 fluorescent dye (Fig.3a-d). Furthermore, slow calcium waves were detectable in the presence of TTX but disappeared when applying thapsigargin (see Fig.4e-f)

In the following experiments neuronal and glial activity was monitored simultaneously: a neuron was patched in the OGB loaded slice in current clamp configuration, and calcium wave changes were detected on 5-21 loaded astrocytes within 50 µm from the soma of the patched neuron.

20

Depolarization exceeding 2 mV in the patched neuron, was accompanied by an increase of astrocytic calcium wave frequency (Fig. 3e) that either preceded (Fig. 3f) or appeared parallel with the onset of neuronal depolarization. Surrounding astrocytes in these cases had initially low frequency spontaneous activity that increased rapidly after application of ACEA, and this two-fold increase existed for approximately 4 minutes (Fig. 3f).

Astrocytes in the vicinity of neurons that were hyperpolarized upon ACEA application also showed an initially low basal calcium wave frequency, which increased during ACEA administration slightly preceding the neuronal hyperpolarization. Calcium wave frequency increase in this case was not transient but kept increasing gradually and reached a higher value than the maximum frequency of astrocytes around depolarizing neurons (Fig.3g-h)

Interestingly, initial astrocytic calcium wave frequency was high around neurons that were unaffected by ACEA and calcium wave frequency increase in these astrocytes was not detectable during the application of ACEA (Fig. 3i-j)

CB1 receptors, located on astrocytes, are responsible for neuronal membrane potential changes upon ACEA application

In order to prove that CB1 receptors are located on astrocytes of the PPN we performed immunocytochemistry to demonstrate co-localization of CB1 receptor and glial fibrillary acidic protein (GFAP), a marker for astrocytes. We found that a substantial proportion of astrocytic processes showed immunostaining for CB1 receptor (Fig. 4a-c).

To provide functional evidence that CB1 agonists were activating astrocytes directly through these CB1 receptors, we repeated the combined Ca-imaging and patch-clamp experiments on CB1 knockout mice. Compared to wild type animals, loaded astrocytes showed spontaneous calcium waves at a significantly lower initial frequency. When ACEA was applied, the frequency did not increase significantly (Fig.4d,h). Neurons of the PPN in these animals (n = 13) failed to produce significant membrane potential change during the application of ACEA (see Fig. 1k)

Apart from the direct activation of glial CB1 receptors, astrocytic activation might also occur via indirect mechanisms initiated by altered neuronal activity. To test this possibility, tetrodotoxin (TTX) was applied to suspend neuronal action potential firing in slices from wild type mice. In the presence of TTX calcium wave frequency in loaded astrocytes was significantly lower than in control conditions (Fig. 4e,h). However, when ACEA was applied, a significant increase of calcium wave frequency was observed. (Fig.4h).

Next, we wanted to test whether silencing of astrocytes can prevent neuronal membrane potential changes in response to CB1 receptor agonists. Slices from wild type mice were incubated with thapsigargin (1 µM), a drug depleting intracellular calcium stores (Navarrete and Araque, 2008, 2010), for 45 minutes prior to the 10-minute-long registration. Intracellular calcium concentration of the patched neuron was set by the pipette solution. After preincubation with thapsigargin, as expected, no astrocytic slow calcium waves were observed (n = 58; Fig. 4f,h) and neuronal responses to ACEA were limited to negligible hyperpolarization or did not show changes (n = 7; Fig. 4g). The pattern of resting membrane potential change in response to ACEA application was

significantly different compared to control conditions (Fig.4g). The lack of neuronal response was not related to the general inhibition of the neuron by thapsigargin, since application of 10 μM glutamate resulted in 9.43 ± 4.9 mV depolarization and 1.64 ± 1.05 Hz increase of the firing frequency (n = 4; not shown).

Effect of CB1 agonists depend on basal neuronal and glial activity

In the next set of experiments we analyzed why membrane potential changes are missing in some neurons during ACEA application (see Fig.3i-j) and if this absence of response is related to the basal activity of neurons. We found, that the magnitude of the response to ACEA was inversely proportional to the initial firing frequency: larger changes of membrane potential were associated with lower initial firing frequencies (or no firing) while membrane potential of cells exhibiting high initial firing rate was almost unaffected by ACEA (Fig.5a). Similarly, glial cells with originally low calcium wave frequency displayed a higher frequency increase to ACEA (Fig.5b).

One possible explanation for this inverse relationship could be that a locally increased endocannabinoid tone prevents the action of ACEA. Thus, we incubated the slices with a lower concentration of ACEA (50 nM) for 5-7 minutes before application of 5 μM ACEA. Under these conditions changes of neuronal resting membrane potential were significantly lower (n = 15; Fig.5c-d). Initial astrocyte calcium wave frequency was higher than in control conditions (i.e. without the low concentration of ACEA, see Fig.3e and g). Similarly to astrocytes surrounding the non-responding neurons (see Fig.3i), spontaneously active loaded astrocytes incubated with 50 nM ACEA did not increase their calcium wave frequency to the further application of 5 μM ACEA (Fig.5c,d).

Finally, evidence was sought whether, similarly to synthetic cannabinoid agonist application, endocannabinoid release from the spontaneously or otherwise discharging neurons can lead to astrocyte calcium wave frequency increase. In parallel with a 10 mV depolarization (30 s period) of neurons (n = 3) from wild type animals astrocytes within 50 μm from the neuronal soma almost doubled their calcium wave frequency (Fig. 6a-c). In case of neurons from CB1 receptor knockout animals (n = 4) this change in the calcium wave frequency was significantly smaller (Fig 6d-f).

Discussion

In this study we present evidence that cannabinoids have an indirect heterogeneous effect on PPN neurons. The mechanism requires the presence of astrocytes with functional CB1 receptors. Summarizing our results, we propose the following scheme of endocannabinoid modulation within the PPN. Neurons that are spontaneously or otherwise active synthesize and release endocannabinoids that activate neighboring astrocytes via CB1 receptors. This activation leads to consequential gliotransmitter release, in this particular case, glutamate. The released glutamate will depolarize PPN neurons with group II mGluR receptors and hyperpolarize the ones that express group I mGluRs (Fig. 7).

Activation of CB1 receptors on astrocytes leads to modulation of neuronal activities in the PPN.

It is a well-accepted fact that astrocytes are able to modulate neuronal functions effectively (Perea et al., 2009; Frank, 2013.) They possess several functional neurotransmitter receptors through which they can be activated in a specific way and release several gliotransmitters, such as glutamate, ATP, adenosine, TNFα, peptides (Volterra and Bezzi, 2002). Astrocytes, for example, directly contribute to sleep homeostasis (reviewed by Frank, 2013) via the release of IL-1, TNFα, neurotrophins and prostaglandins. One of the most extensively investigated gliotransmitter, glutamate, is released by astrocytes in multiple ways: besides calcium-dependent exocytosis (Parpura et al., 1994; Bezzi et al., 2004), reversal of uptake by plasma membrane glutamate

transporters (Szatkowski et al., 1990), cystine-glutamate antiport (Warr et al., 1999), functional unpaired connexon/pannexon "hemichannels" (Cotrina et al., 1998; Ye et al., 2003), ionotropic purinergic receptors (Duan et al., 2003), organic anionic transporters (Rosenberg et al., 1994) and cell swelling induced anion channel opening (Pasantes Morales and Schousboe, 1988) were also reported.

Several studies revealed that both cultured astrocytes (Molina-Holgado et al., 2003, Stella, 2004, Walter and Stella, 2003) and astrocytes of certain brain regions, such as the nucleus accumbens, cingulate cortex, medial forebrain bundle, amygdala, spinal cord and hippocampus (Rodríguez et al., 2001; Moldrich and Wenger, 2000; Salio et al., 2002; Navarrete and Araque, 2008; Hegyi et al., 2009) possess CB1 receptors and respond to cannabinoids with calcium waves (Navarrete and Araque, 2008). The presence of functional CB2 receptor on astrocytes is also well established (e.g. Fernandez-Ruiz et al, 2008), but the contribution of this receptor to the effects observed by us is not likely for two reasons: ACEA is thought to be highly selective to CB1 receptor (Hillard et al, 1999) and the effects of ACEA and WIN55,212-2 were almost completely absent on CB1 receptor knockout mice.

The role of astrocytes in cannabinoid signaling of the hippocampus and barrel cortex was recently demonstrated (Navarrete and Araque, 2008, 2010; Min and Nevian, 2012; Han et al., 2012; Coiret et al., 2012; Castillo et al., 2012). In these regions increased neuronal activity leads to endocannabinoid release that activates astrocytes that respond by releasing glutamate. Glutamate can either potentiate glutamatergic synapses or initiate long term depression in NMDA receptor or presynaptic mGluR dependent ways. In this present work, we provide the first evidence that a similar, although not

identical mechanism is also present in a subcortical nucleus of the reticular activating system. We showed that –similar to the cortical structures (Navarrete and Araque, 2008, 2010; Castillo et al., 2012)- activation of neurons lead to the consequential activation of the astrocytes, mostly via CB1 receptor and that astrocyte activation leads to glutamate release, which acts on metabotropic glutamate receptors. However, in case of the system that we revealed potentiation of the EPSCs by astrocytic glutamate release does not seem to be the main factor altering membrane potential of neurons of the PPN, as blockade of ionotropic glutamate receptors failed to cause significant changes in the effect of CB1 receptor stimulation on neuronal membrane potential.

The role of mGluRs in glia-neuron signaling.

Our pharmacological tests with blockers of group I and II mGluRs suggest that hyperpolarization is due to the activation of postsynaptic group I mGluRs, whereas depolarization depends on group II mGluRs. Recent studies demonstrated the presence and function of group I and II mGluRs in certain midbrain regions (Wilson-Poe et al., 2013; Kohlmeier et al., 2013) and activation of astrocytes leading to consequential stimulation of presynaptic mGluRs and contribution to long term potentiation in the hippocampus (Navarrete et al., 2012) has also been described. However, to the best of our knowledge, this study is the first that indicates indirect stimulation of different classes of postsynaptic mGluRs by activation of astrocytic CB1 receptors in the midbrain.

Metabotropic glutamate receptors are present in a wide variety of locations in the central nervous system; where they are also present in both pre- and postsynaptic

locations and on astrocytes as well (e.g. Ferraguti and Shigemoto, 2006; Niswender and Conn, 2010).

It is well established that astrocytes possess both group I and II mGluRs (Petralia et al., 1996; Schools and Kimelberg, 1999; Zur Nieden and Deitmer, 2006; D'Ascenzo et al, 2007; Pirttimaki and Parri, 2012; Ferraguti and Shigemoto, 2006; Schoepp, 2001; D'Antoni et al., 2008), making astrocytes able to sense changes of extracellular glutamate (Zur Nieden and Deitmer, 2006). Glutamate and group I and II mGluR agonists elicited calcium signals in rat hippocampal astrocytes, inducing "glutamate-induced glutamate release" (Bezzi et al., 2004; Zur Nieden and Deitmer, 2006; Pirttimaki et al, 2011; D'Ascenzo et al, 2007). In contrast, blockers of group I and II mGluRs failed to change parameters of spontaneous calcium oscillations in mouse hippocampal astrocytes (Nett et al, 2002).

Several authors referred that activation of postsynaptic group I and II mGluRs lead to changes of the neuronal membrane potential.

According to numerous studies, activation of postsynaptic group I mGluRs cause depolarization and group II mGluR stimulation leads to hyperpolarization (see Sherman, 2014). Group I mGluR stimulation depolarized neurons (Libri et al., 1997; Partridge et al, 2014) via activation of L-type calcium channel on CA1 pyramidal cells (Kato et al, 2012) and in the cingulate cortex (Zhang and Seguela, 2010), or a non-selective cationic conductance on olfactory granule cells (Smith et al., 2009). Activation of group II mGluRs either suppress L-type calcium channel (Chavis et al, 1994; 1995) or activate potassium channels (Knoflach and Kemp, 1998; Irie et al, 2006; Hermes and Renaud, 2011), thus hyperpolarizing the neurons expressing them.

However, the opposite effects were also observed. In cortical and subcortical structures (hippocampus, amygdala, olfactory bulb, pallidum, laterodorsal tegmental nucleus) stimulation of postsynaptic mGluR5 (belonging to the group I mGluRs) lead to the activation of K^+ channels (Jian et al., 2010; Mannaioni et al., 2001; Poisik et al, 2003; Rainnie et al., 1994; Harata et al., 1996; Kohlmeier et al. 2013), which hyperpolarized the neurons expressing the receptor. Activation of group II mGluRs in somatodendritic location caused a postsynaptic excitatory response in hippocampal CA3 pyramidal cells by activating a cationic conductance and inhibiting a potassium conductance (Ster et al., 2011).

In our project, blockers of group I mGluRs prevented ACEA-induced hyperpolarization and the group II. mGluR antagonist inhibited depolarization. Blockade of ionotropic glutamate receptors failed to change the effect of ACEA on the resting membrane potential, whereas glutamate was capable of causing neuronal depolarization in the presence of thapsigargin. These results indicate that astrocytic activation by CB1 receptor agonists, different groups of metabotropic glutamate receptors and neuronal responses to glutamate are important for the observed multiple effects of cannabinoids. Based on our data, the simplest model is where endocannabinoids released by neurons activate astrocytes via the CB1 receptor. Astrocytes, in turn, release glutamate and depolarize or hyperpolarize surrounding neurons by activating different groups of mGluRs on them (Fig. 7).

However, the proposed model might oversimplify the situation. Astrocytes are known to express different mGluRs (Zur Nieden and Deitmer, 2006) leading to functional differences between astrocytes based on the presence or absence of certain

mGluRs (Parri et al, 2010). We observed differences in the time scale and magnitude of astrocytic response to ACEA around depolarized and hyperpolarized neurons (Fig. 3f, h). This might indicate that distinct groups of astrocytes have different mGluRs, which could be responsible for prolongation of glutamate actions by "glutamate-induced glutamate release" (D'Ascenzo et al, 2007), increase or decrease of tonic glutamate release (Xi et al, 2002; Zur Nieden and Deitmer, 2006), or release of glutamate co-released with another gliotransmitter from different groups of astrocytes (Shibasaki et al, 2014).

We also showed that an increased endocannabinoid tone may be responsible for the absence or reduction of neural and astrocytic response to ACEA. However, other activity-dependent or cell type specific mechanisms might also be responsible for this later phenomenon, as preincubation of slices with low dose of ACEA could not mimic fully the non-responsiveness of cells with initially high activity level.

The heterogeneous response of PPN neurons to CB1 receptor stimulation might contribute to the reported effects of exogenous and endocannabinoids on sleep.

Cannabinoid receptor agonists are known to increase the duration of REM sleep (Murillo-Rodriguez et al., 1998, 2001, 2008; Murillo-Rodriguez, 2008; Herrera-Solís et al., 2010) and non-REM sleep (Herrera-Solís et al., 2010; Bolla et al., 2008). Although correlating our in vitro data with in vivo observations might be speculative, we believe that the modulatory effect of endocannabinoids on PPN neurons, reported in this paper, might contribute to physiological and pathophysiological mechanism through which, endo- and exogenous cannabinoids increase REM and non-REM sleep duration (Feinberg

et al., 1975; Murillo-Rodriguez et al., 1998, 2008; Murillo-Rodriguez, 2008; Herrera-Solís et al., 2010).

In correlation with cortical slow wave activity, the majority of cholinergic cells fire at the active phase, whereas a subset of non-cholinergic cells discharges during the inactive phase. When cortical gamma activity is present, the majority of cholinergic neurons increase firing rate and only a fast firing minority lack changes, whereas certain subgroups of non-cholinergic neurons increase, decrease or do not change their firing rate (Mena-Segovia et al., 2008; Ros et al., 2010). In line with the above, our study revealed similar cell type specific differences of the cannabinoid effect. Although both cholinergic and GABAergic cells showed all three types of responses, a substantial part (one-third) of the cholinergic neurons did not respond to CB1 receptor stimulation. These neurons all had relatively high initial firing frequency (4-6 Hz), indicating that they might belong to the group of "fast-firing cholinergic" cells (Mena-Segovia et al., 2008), which do not increase firing rate during cortical gamma activity. Depolarization, on the other hand, dominated (70%) among the GABAergic cells. Interestingly, in vivo observations showed that a proportion of non-cholinergic neurons with quiescent and irregular firing pattern were activated in time with cortical gamma oscillations, whereas neurons with tonic firing pattern did not change (Ros et al., 2010). It is possible, that the majority of our GABAergic cells belong to these quiescent or irregular cells observed by Ros et al. (2010). The single GABAergic neuron in our sample that showed tonic activity with a higher firing rate did not respond to ACEA.

Although the PPN also contains glutamatergic neurons, we did not investigate this population. However, based on the similarities between the GAD65-positive and non-

31

cholinergic populations –which theoretically includes both GABAergic and glutamatergic neurons-, one can assume that glutamatergic neurons might have a response similar to that of the GABAergic ones.

Based on the in vivo data, one might hypothesize that REM sleep associated with cortical desynchronization (e.g. Pace-Schott, 2009; Steriade et al., 1990) requires an increased firing rate from the majority of cholinergic cells and a subset of GABAergic cells, along with inhibition of a small population of irregular firing GABAergic neurons, while fast firing cholinergic and tonic firing GABAergic neurons do not change their activity (Mena-Segovia et al., 2008; Ros et al., 2010). In contrast with these expectations, our findings show that only one-third of the cholinergic neurons were activated by ACEA, while the other two-thirds were hyperpolarized or lacked response to CB1 receptor stimulation. The majority of the GABAergic neurons were activated by ACEA and only a minor population lacked response or became hyperpolarized.

This contradiction may be explained in several ways. First, according to some studies (Murillo-Rodriguez et al., 2001; Herrera-Solís et al., 2010; Bolla et al., 2008) cannabinoids increased the duration of both REM- and non-REM sleep; thus, it might be the case that depending on the actual combination of PPN neuronal responses, different phases of sleep will be effected by cannabinoids. Second, it is well established that the proportion of REM- and non-REM sleep from the total duration of sleep is changing with age (Tarokh and Carskadon, 2009). In rats, it reaches its maximum around the 10th postnatal day, and shows a gradual decrease until the proportion characteristic for adulthood is established around the 30th postnatal day. These changes are concomitant with changes of membrane potential by stimulation of different receptors (NMDA,

kainate, M2, GABAA and B, 5-HT1, etc.; reviewed by Garcia-Rill et al., 2008). Age-related changes of the expression level of CB1 receptor and metabotropic glutamate receptors were also shown in other structures (e.g. Hubert and Smith, 2004; Díaz-Alonso et al, 2014). Therefore, the conditions we explored can be applicable for younger ages characterized by an increased REM sleep duration.

Finally, our in vitro approach investigates a network that lacks important modulating input and the influence of global brain activity. Thus neurons in this slice preparation most likely reflect the first step in the complex modulating effects of cannabinoids that may look different in the complete system. Nevertheless, this approach is ideal for dissecting the pharmacological interplay between cellular elements of the PPN.

In summary, we provided evidence that PPN neurons change their membrane potential and action potential firing frequency in a heterogeneous way to CB1 receptor stimulation, via activation of astrocytic CB1 receptors. This indirect cannabinoid signaling pathway seems to regulate the PPN neurons effectively, and most likely provides an important contribution to its oscillatory activity determining global brain states.

References

Bezzi P, Gundersen V, Galbete JL, Seifert G, Steinhäuser C, Pilati E, Volterra A (2004) Astrocytes contain a vesicular compartment that is competent for regulated exocytosis of glutamate. Nat Neurosci. 7(6):613-20.

Bolla KI, Lesage SR, Gamaldo CE, Neubauer DN, Funderburk FR, Cadet JL, David PM, Verdejo-Garcia A, Benbrook AR. (2008) Sleep disturbance in heavy marijuana users. Sleep. 31(6):901-8.

Castillo PE, Younts TJ, Chávez AE, Hashimotodani Y. (2012) Endocannabinoid signaling and synaptic function. Neuron, 76(1): 70-81.

Chavis P, Shinozaki H, Bockaert J, Fagni L (1994) The metabotropic glutamate receptor types 2/3 inhibit L-type calcium channels via a pertussis toxin-sensitive G-protein in cultured cerebellar granule cells. J Neurosci. 14(11 Pt 2):7067-76.

Chavis P, Fagni L, Bockaert J, Lansman JB (1995) Modulation of calcium channels by metabotropic glutamate receptors in cerebellar granule cells. Neuropharmacology. 34(8):929-37.

Coiret G, Ster J, Grewe B, Wendling F, Helmchen F, Gerber U, Benquet P. (2012) Neuron to astrocyte communication via cannabinoid receptors is necessary for sustained epileptiform activity in rat hippocampus. PLoS One. 7(5):e37320.

Cotrina ML, Lin JH, Alves-Rodrigues A, Liu S, Li J, Azmi-Ghadimi H, Kang J, Naus CC, Nedergaard M. (1998) Connexins regulate calcium signaling by controlling ATP release. Proc Natl Acad Sci U S A. 95(26):15735-40.

D'Antoni S, Berretta A, Bonaccorso CM, Bruno V, Aronica E, Nicoletti F, Catania MV (2008) Metabotropic glutamate receptors in glial cells. Neurochem Res. 33(12):2436-43.

D'Ascenzo M, Fellin T, Terunuma M, Revilla-Sanchez R, Meaney DF, Auberson YP, Moss SJ, Haydon PG (2007) mGluR5 stimulates gliotransmission in the nucleus accumbens. Proc Natl Acad Sci U S A. 104(6):1995-2000.

Díaz-Alonso J, Aguado T, de Salas-Quiroga A, Ortega Z, Guzmán M, Galve-Roperh I (2014) CB1 Cannabinoid Receptor-Dependent Activation of mTORC1/Pax6 Signaling Drives Tbr2 Expression and Basal Progenitor Expansion in the Developing Mouse Cortex. Cereb Cortex. 2014 Mar 7.

Duan S, Anderson CM, Keung EC, Chen Y, Chen Y, Swanson RA. (2003) P2X7 receptor-mediated release of excitatory amino acids from astrocytes. J Neurosci. 23(4):1320-8.

Feinberg I, Jones R, Walker JM, Cavness C, March J (1975) Effects of high dosage delta-9-tetrahydrocannabinol on sleep patterns in man. Clin Pharmacol Ther 17(49): 458-466.

Fernández-Ruiz J, Pazos MR, García-Arencibia M, Sagredo O, Ramos JA (2008) Role of CB2 receptors in neuroprotective effects of cannabinoids. Molecular and Cellular Endocrinology 286(1-2) Supplement 1, S91-S96

Ferraguti F, Shigemoto R (2006) Metabotropic glutamate receptors. Cell Tissue Res. 326(2):483-504.

Frank MG. (2013) Astroglial regulation of sleep homeostasis. Curr Opin Neurobiol. 23(5):812-8.

Garcia-Rill E (1991) The pedunculopontine nucleus. Prog Neurobiol 36: 363-389.

Garcia-Rill E, Charlesworth A, Heister D, Ye M, Hayar A. (2008) The developmental decrease in REM sleep: the role of transmitters and electrical coupling. Sleep. 31(5):673-90.

Garcia-Rill E, Simon C, Smith K, Kezunovic N, Hyde J (2011) The pedunculopontine tegmental nucleus: from basic neuroscience to neurosurgical applications. J Neural Transm 118: 1397 – 1407.

Han J, Kesner P, Metna-Laurent M, Duan T, Xu L, Georges F, Koehl M, Abrous DN, Mendizabal-Zubiaga J, Grandes P, Liu Q, Bai G, Wang W, Xiong L, Ren W, Marsicano G, Zhang X. (2012) Acute cannabinoids impair working memory through astroglial CB1 receptor modulation of hippocampal LTD. Cell. 148(5): 1039-50.

Harata N, Katayama J, Takeshita Y, Murai Y, Akaike N (1996) Two components of metabotropic glutamate responses in acutely dissociated CA3 pyramidal neurons of the rat. Brain Res 711: 223-233.

Hegyi Z, Kis G, Holló K, Ledent C, Antal M (2009) Neuronal and glial localization of the cannabinoid-1 receptor in the superficial spinal dorsal horn of the rodent spinal cord. Eur J Neurosci, 30(2): 251-62.

Hegyi Z, Holló K, Kis G, Mackie K, Antal M (2012) Differential distribution of diacylglycerol lipase-alpha and N-acylphosphatidylethanolamine-specific phospholipase d immunoreactivity in the superficial spinal dorsal horn of rats. Glia 60(9): 1316-29

Hermes ML, Renaud LP (2011) Postsynaptic and presynaptic group II metabotropic glutamate receptor activation reduces neuronal excitability in rat midline paraventricular thalamic nucleus. J Pharmacol Exp Ther. 336(3):840-9.

Herrera-Solís A, Vásquez KG, Prospéro-García O (2010) Acute and subchronic administration of anandamide or oleamide increases REM sleep in rats. Pharmacology, Biochemistry and Behaviour 95: 106-112.

Hillard CJ, Manna S, Greenberg MJ, DiCamelli R, Ross RA, Stevenson LA, Murphy V, Pertwee RG, Campbell WB (1999) Synthesis and characterization of potent and selective agonists of the neuronal cannabinoid receptor (CB1). J Pharmacol Exp Ther. 289(3):1427-33.

Hubert GW, Smith Y (2004) Age-related changes in the expression of axonal and glial group I metabotropic glutamate receptor in the rat substantia nigra pars reticulata. J Comp Neurol. 2004 475(1):95-106.

Irie T, Fukui I, Ohmori H (2006) Activation of GIRK channels by muscarinic receptors and group II metabotropic glutamate receptors suppresses Golgi cell activity in the cochlear nucleus of mice. J Neurophysiol. 96(5):2633-44.

Jenkinson N, Nandi D, Muthusamy K, Ray NJ., Gregory R, Stein JF, Aziz TZ (2009) Anatomy, physiology, and pathophysiology of the pedunculopontine nucleus. Movement Disorders 24(3): 319-328.

Jian K, Cifelli P, Pignatelli A, Frigato E, Belluzzi O (2010) Metabotropic glutamate receptors 1 and 5 differentially regulate bulbar dopaminergic cell function. Brain Res. 1354:47-63.

Kato HK, Kassai H, Watabe AM, Aiba A, Manabe T. (2012) Functional coupling of the metabotropic glutamate receptor, InsP3 receptor and L-type Ca2+ channel in mouse CA1 pyramidal cells. J Physiol. 590(Pt 13):3019-34.

Katona I, Sperlágh B, Sík A, Kőfalvi A, Vizi ES, Mackie K, Freund TF (1999) Presynaptically located CB1 cannabinoid receptors regulate GABA release from axon terminals of specific hippocampal interneurons. J Neurosci 19: 4544–4558.

Katona I, Freund TF (2012) Multiple functions of endocannabinoid signaling in the brain. Annu Rev Neurosci 35: 529-558.

Kawamura Y, Fukaya M, Maejima T, Yoshida T, Miura E, Watanabe M, Ohno-Shosaku T, Kano M (2006) The CB1 cannabinoid receptor is the major cannabinoid receptor at excitatory presynaptic sites in the hippocampus and cerebellum. J Neurosci, 26, 2991–3001.

Knoflach F, Kemp JA (1998) Metabotropic glutamate group II receptors activate a G protein-coupled inwardly rectifying K+ current in neurones of the rat cerebellum. J Physiol. 509 (Pt 2):347-54.

Kohlmeier KA, Christensen MH, Kristensen MP, Kristiansen U (2013) Pharmacological evidence of functional inhibitory metabotrophic glutamate receptors on mouse arousal-related cholinergic laterodorsal tegmental neurons. Neuropharmacology 66: 99-113.

Kőszeghy Á, Vincze J, Rusznák Z, Fu Y, Paxinos G, Csernoch L, Szücs G (2012) Activation of muscarinic receptors increases the activity of the granule neurons of the rat dorsal cochlear nucleus--a calcium imaging study. Pflugers Arch 463(6): 829-44.

Libri V, Constanti A, Zibetti M, Postlethwaite M (1997) Metabotropic glutamate receptor subtypes mediating slow inward tail current (IADP) induction and inhibition of synaptic transmission in olfactory cortical neurones. Br J Pharmacol. 120(6):1083-95.

Madisen L, Zwingman TA, Sunkin SM, Oh SW, Zariwala HA, Gu H, Ng LL, Palmiter RD, Hawrylycz MJ, Jones AR, Lein ES, Zeng H (2010) A robust and high-throughput Cre reporting and characterization system for the whole mouse brain. Nat Neurosci. 13(1): 133-40.

Maloney K, Mainville L, Jones BE (1999) Differential c-Fos expression in cholinergic, monoaminergic, and GABAergic cell groups of the pontomesencephalic tegmentum after paradoxical sleep deprivation and recovery. J Neurosci 19(8): 3057-3072.

Mannaioni G1, Marino MJ, Valenti O, Traynelis SF, Conn PJ (2001) Metabotropic glutamate receptors 1 and 5 differentially regulate CA1 pyramidal cell function. J Neurosci. 21(16):5925-34.

Mena-Segovia J, Sims HM, Magill PJ, Bolam JP (2008) Cholinergic brainstem neurons modulate cortical gamma activity during slow oscillations. J Physiol 586.12: 2947-2960.

Min R., Nevian T (2012) Astrocyte signaling controls spike timing-dependent depression at neocortical synapses. Nat Neurosci. 15(5):746-53.

Moldrich G, Wenger T. (2000) Localization of the CB1 cannabinoid receptor in the rat brain. An immunohistochemical study. Peptides. 21(11):1735-42.

Molina-Holgado F, Pinteaux E, Moore JD, Molina-Holgado E, Guaza C, Gibson RM, Rothwell NJ. (2003) Endogenous interleukin-1 receptor antagonist mediates anti-inflammatory and neuroprotective actions of cannabinoids in neurons and glia. J Neurosci. 23(16):6470-4.

Murillo-Rodríguez E, Sánchez-Alavez M, Navarro L, Martínez-González D, Drucker-Colín R, Prospéro-García O. (1998) Anandamide modulates sleep and memory in rats. Brain Res 812(1-2): 270-4.

Murillo-Rodríguez E, Cabeza R, Méndez-Díaz M, Navarro L, Prospéro-García O. (2001) Anandamide-induced sleep is blocked by SR141716A, a CB1 receptor antagonist and by U73122, a phospholipase C inhibitor. Neuroreport. 12(10):2131-6.

Murillo-Rodriguez E. (2008) The role of the CB1 receptor in the regulation of sleep. Progress in Neuro-Psychopharmacology and Biological Psychiatry 32: 1420-1427.

Murillo-Rodriguez E, Millán-Aldaco D, Di Marzo V, Drucker-Colín R (2008) The anandamide membrane transporter inhibitor VDM-11, modulates sleep and c-Fos expression in the rat brain. Neuroscience 157: 1-11.

Navarrete M, Araque A (2008)   Endocannabinoids mediate neuron-astrocyte communication. Neuron 58: 883-893.

Navarrete M, Araque A (2010) Endocannabinoids potentiate synaptic transmission through stimulation of astrocytes. Neuron 68: 113 – 126.

Navarrete M, Perea G, Fernandez de Sevilla D, Gómez-Gonzalo M, Núnez A, Martín ED, Araque A (2012) Astrocytes mediate in vivo cholinergic-induced synaptic plasticity. PLoS Biology 10(2): e1001259.

Nett WJ, Oloff SH, McCarthy KD (2002) Hippocampal astrocytes in situ exhibit calcium oscillations that occur independent of neuronal activity. J Neurophysiol. 87(1):528-37.

Nimmerjahn A, Kirchhoff F, Kerr JN, Helmchen F (2004)   Sulforhodamine 101 as a specific marker of astroglia in the neocortex in vivo. Nat Methods 1:31-37.

Niswender CM, Conn PJ (2010) Metabotropic glutamate receptors: physiology, pharmacology, and disease. Annu Rev Pharmacol Toxicol. 50:295-322.

Pace-Schott EF (2009) Sleep architecture. In: The neuroscience of sleep. (Stickgold R, Walker M, ed), pp10-17. Elsevier.

Parpura V, Basarsky TA, Liu F, Jeftinija K, Jeftinija S, Haydon PG. (1994) Glutamate-mediated astrocyte-neuron signalling. Nature. 369(6483):744-7.

Parri HR, Gould TM, Crunelli V (2010) Sensory and cortical activation of distinct glial cell subtypes in the somatosensory thalamus of young rats. Eur J Neurosci. 32(1):29-40.

Partridge JG, Lewin AE, Yasko JR, Vicini S (2014) Contrasting actions of Group I metabotropic glutamate receptors in distinct mouse striatal neurones. J Physiol. 2014 Apr 7.

Pasantes Morales H, Schousboe A. (1988) Volume regulation in astrocytes: a role for taurine as an osmoeffector. J Neurosci Res. 20(4):503-9.

Paxinos G, Franklin KBJ (2004) The mouse brain atlas in stereotaxic coordinates. Elsevier, USA.

Perea G, Navarrete M, Araque A. (2009) Tripartite synapses: astrocytes process and control synaptic information. Trends Neurosci. 32(8):421-31.

Petralia RS, Wang YX, Niedzielski AS, Wenthold RJ (1996) The metabotropic glutamate receptors, mGluR2 and mGluR3, show unique postsynaptic, presynaptic and glial localizations. Neuroscience. 71(4):949-76.

Pirttimaki TM, Hall SD, Parri HR (2011) Sustained neuronal activity generated by glial plasticity. J Neurosci. 31(21):7637-47.

Pirttimaki TM, Parri HR (2012) Glutamatergic input-output properties of thalamic astrocytes. Neuroscience. 205:18-28.

Poisik OV, Mannaioni G, Traynelis S, Smith Y, Conn PJ (2003) Distinct functional roles of the metabotropic glutamate receptors 1 and 5 in the rat globus pallidus. J Neurosci. 23(1):122-30.

Rainnie DG, Holmes KH, Shinnick-Gallagher P (1994) Activation of postsynaptic metabotropic glutamate receptors by trans-ACPD hyperpolarizes neurons of the basolateral amygdala. J Neurosci 14: 7208-7220.

Reese NB, Garcia-Rill E, Skinner RD (1995) The pedunculopontine nucleus - auditory input, arousal and pathophysiology. Prog Neurobiol 42: 105-133.

Rodriguez JJ, Mackie K, Pickel VM. (2001) Ultrastructural localization of the CB1 cannabinoid receptor in mu-opioid receptor patches of the rat Caudate putamen nucleus. J Neurosci. 21(3):823-33.

Rodriguez-Cueto C, Benito C, Fernández-Ruiz J, Romero J, Hernández-Gálvez M, Gómez-Ruiz M. (2013) Changes in Cb_1 and Cb_2 Receptors in the Postmortem Cerebellum of Humans Affected by Spinocerebellar Ataxias. Br J Pharmacol. doi: 10.1111/bph.12283.

Ros H, Magill PJ, Moss J, Bolam JP, Mena-Segovia J (2010) Distinct types of non-cholinergic pedunculopontine neurons are differentially modulated during global brain states. Neuroscience 170: 78-91.

Rosenberg PA, Knowles R, Knowles KP, Li Y. (1994) Beta-adrenergic receptor-mediated regulation of extracellular adenosine in cerebral cortex in culture. J Neurosci. 14(5 Pt 2):2953-65.

Salio C, Doly S, Fischer J, Franzoni MF, Conrath M. (2002) Neuronal and astrocytic localization of the cannabinoid receptor-1 in the dorsal horn of the rat spinal cord. Neurosci Lett. 329(1):13-6.

Schoepp DD (2001) Unveiling the functions of presynaptic metabotropic glutamate receptors in the central nervous system. J Pharmacol Exp Ther 299(1):12-20.

Schools GP, Kimelberg HK (1999) mGluR3 and mGluR5 are the predominant metabotropic glutamate receptor mRNAs expressed in hippocampal astrocytes acutely isolated from young rats. J Neurosci Res. 58(4):533-43.

Sherman SM (2014) The function of metabotropic glutamate receptors in thalamus and cortex. Neuroscientist. 20(2):136-49.

Shibasaki K, Ikenaka K, Tamalu F, Tominaga M, Ishizaki Y. (2014) A novel subtype of astrocytes expressing TRPV4 regulates neuronal excitability via release of gliotransmitters. J Biol Chem. 2014 Apr 15.

Smith RS, Weitz CJ, Araneda RC (2009) Excitatory actions of noradrenaline and metabotropic glutamate receptor activation in granule cells of the accessory olfactory bulb. J Neurophysiol. 102(2):1103-14.

Stella N. (2004) Cannabinoid signaling in glial cells. Glia. 48(4):267-77.

Ster J, Mateos JM, Grewe BF, Coiret G, Corti C, Corsi M, Helmchen F, Gerber U (2011) Enhancement of CA3 hippocampal network activity by activation of group II metabotropic glutamate receptors. Proc Natl Acad Sci U S A. 108(24):9993-7.

Steriade M, Datta S, Paré D, Oakson G, Curró Dossi RC (1990) Neuronal activities in brain-stem cholinergic nuclei related to tonic activation processes in thalamocortical systems. J Neurosci 10(8):2541-59.

Szatkowski M, Barbour B, Attwell D. (1990) Non-vesicular release of glutamate from glial cells by reversed electrogenic glutamate uptake. Nature. 348(6300):443-6.

Taniguchi H, He M, Wu P, Kim S, Paik R, Sugino K, Kvitsiani D, Fu Y, Lu J, Lin Y, Miyoshi G, Shima Y, Fishell G, Nelson SB, Huang ZJ (2011) A resource of Cre driver lines for genetic targeting of GABAergic neurons in cerebral cortex. Neuron 71(6): 995-1013.

Tarokh L, Carskadon MA (2009) Sleep in adolescents. In: The neuroscience of sleep (Stickgold R, Walker M, ed), pp. 70-77. Elsevier.

Volterra A, Bezzi P (2002) Chapter 13: Release of transmitters from glial cells. In The tripartite synapse: Glia in Synaptic Neurotransmission (Volterra, A. et al., eds), pp. 164-184, Oxford University Press.

Walter L, Stella N. (2003) Endothelin-1 increases 2-arachidonoyl glycerol (2-AG) production in astrocytes. Glia. 44(1):85-90.

Warr O, Takahashi M, Attwell D. (1999) Modulation of extracellular glutamate concentration in rat brain slices by cystine-glutamate exchange. J Physiol. 514 (Pt 3):783-93.

Wilson RI, Nicoll RA (2001) Endogenous cannabinoids mediate retrograde signaling at hippocampal synapses. Nature, 410: 588–592.

Wilson-Poe AR, Mitchell VA, Vaughan CW. (2013) Postsynaptic mGluR mediated excitation of neurons in midbrain periaqueductal grey. Neuropharmacology. 66:348-54.

Winn P (2006) How best to consider the structure and function of the pedunculopontine tegmental nucleus: evidence from animal studies. J Neurol Sci 248: 234-250.

Xi ZX, Baker DA, Shen H, Carson DS, Kalivas PW (2002) Group II metabotropic glutamate receptors modulate extracellular glutamate in the nucleus accumbens. J Pharmacol Exp Ther. 300(1):162-71.

Ye ZC, Wyeth MS, Baltan-Tekkok S, Ransom BR. (2003) Functional hemichannels in astrocytes: a novel mechanism of glutamate release. J Neurosci. 23(9):3588-96.

Zhang Z, Séguéla P (2010) Metabotropic induction of persistent activity in layers II/III of anterior cingulate cortex. Cereb Cortex. 20(12):2948-57.

Zimmer A, Zimmer AM, Hohmann AG, Herkenham M, Bonner TI. (1999) Increased mortality, hypoactivity, and hypoalgesia in cannabinoid CB1 receptor knockout mice. Proc Natl Acad Sci U S A. 96(10):5780-5.

Zur Nieden R, Deitmer JW (2006) The role of metabotropic glutamate receptors for the generation of calcium oscillations in rat hippocampal astrocytes in situ. Cereb Cortex. 16(5):676-87.

Figure legends

Fig. 1. The CB1 receptor agonist ACEA elicits heterogeneous responses on PPN neurons. **a.** Schematic drawing of a coronal midbrain slice (based on Paxinos, 2004). The area of panel b is indicated by a black square. (PPN = pedunculopontine nucleus, LDTg = laterodorsal tegmental nucleus, LDTgV = laterodorsal tegmental nucleus, ventral part) **b.** Micrograph illustrating the distribution of tdTomato-expressing cholinergic neurons in a 200 micron thick section of the mesencephalon. Arrowheads are pointing to the PPN on both sides of the midbrain section. Scale bar: 500 µm. **c.** Drawing of a biocytin-labeled PPN neuron located dorsal from the superior cerebellar peduncle (scp, dashed line). Scale bar: 100 µm. **d-f.** Micrograph of an identified cholinergic neuron. **d.** Biocytin labeling, **e.** tdTomato expressed in a ChAT-dependent way, **f.** merged image. **g-i.** Micrograph of an identified GABAergic neuron. **g.** Biocytin labeling, **h.** tdTomato expressed in a GAD65-dependent way, **i.** merged image. Scale bar for d-i: 20 µm. **j.** Representative traces of neurons responding to the CB1 receptor agonist ACEA in different ways: depolarization and increase of firing frequency (top), hyperpolarization and decrease of firing frequency (middle), lack of response (bottom). **k.** Summary of all data obtained from wild type mice (black dots; n = 46) and from CB1 receptor knockout mice (red dots; n = 13). The change of the resting membrane potential to ACEA is represented on the X axis while the firing frequency change is on the Y axis.

In the preparations from wild type animals a significant correlation was found (S=0.599, p<0.001) between the change in membrane potential and the change in firing

frequency for control cells, suggesting that these processes are not random changes of the examined parameters but consequences of the drug application. In contrast, only small changes of the membrane potential were revealed in the CB1 knockout samples (absolute values of change: 4.322 ± 0.477 mV in the wild type and 0.838 ± 0.243 mV in the knockout, $p < 0.001$). Most notably, there was no significant correlation between the membrane potential change and the frequency change ($S = -0.259$, $p = 0.382$, suggesting that the changes of the parameters are random fluctuations of the examined parameters.

Fig. 2. Cell type specific differences and pharmacological characterization of the cannabinoid effect on PPN neurons. Neurons responding to CB1 receptor activation under control conditions are represented with gray dots, while cells of a particular type or during application of a particular pharmacon are represented with black dots. Membrane potential change is indicated on the X axis while firing frequency change appears on the Y axis. **a.** Effects of the CB1 receptor agonist ACEA in choline acetyltransferase (ChAT) positive (n = 12) and (**b**) GAD65 positive GABAergic neurons (n = 9). **c.** Preincubation with 1 μM tetrodotoxin (TTX) did not diminish changes of the resting membrane potential by ACEA (n = 13) or (**d**) blockers of fast synaptic neurotransmission (10 μM NBQX, 50 μM D-AP5, 1 μM strychnine, 10 μM bicuculline) did not alter significantly the effect of ACEA on PPN neurons (p = 0.603 for multi-group comparison; n = 24). **e.** ACEA application dominantly depolarized PPN neurons (n = 12) in the presence of group I metabotropic glutamate receptor antagonists (100 μM CPCCOEt, 10 μM MPEP). Under these conditions, the proportion of hyperpolarized cells was

significantly lower than without preincubation of group I mGluR blockers (p = 0.021). **f.** The group II metabotropic glutamate receptor antagonist (10 μM LY341495) mostly prevented the depolarizing effect of ACEA (n = 10) and the overall distribution of membrane potential and firing frequency changes upon ACEA application were significantly different from that of the control condition (p = 0.0111) and from the preincubation with group I mGluR blockers (p = 0.0033). **g.** When applied together, inhibitors of fast synaptic neurotransmission and mGluRs almost fully abolished the effect of ACEA on PPN neurons, resulting in no significant change of the resting membrane potential (p = 0.064) or firing frequency (p = 0.063; n = 7).

Fig. 3. Calcium wave frequency changes in astrocytes neighboring neurons responding differently to ACEA application. **a.** OGB-loaded cells in a slice preparation of the PPN. **b.** Slow calcium waves recorded from the cell indicated with asterisk on panel a. **c.** Membrane potential changes (bottom traces) of the cell labelled with asterisk in response to a current step protocol (top traces). Action potentials were not present even in case of large depolarizing current steps. **d.** Fluorescent micrograph showing the morphology of the recorded cell. **e.** Neuronal depolarization and increase of firing frequency elicited by ACEA (upper trace) accompanied by increased frequency of calcium waves in the neighboring astrocytes (lower traces). **f.** Time course of the neuronal membrane potential (top) and astroglial calcium wave frequency (bottom) changes. Each data point represents the average of 30 seconds. The dashed lines indicate the average of all data points before the application of ACEA Note that the significant increase of astrocytic calcium event

frequency preceded neuronal depolarization, reached a plateau after 1-2 minutes and existed for approximately 4 minutes. The maximal frequency of astrocytic calcium waves during application of ACEA was 0.93 ± 0.27/min (n = 7). **g-h.** Astrocytes in the vicinity of neurons hyperpolarizing to ACEA also increased their calcium wave frequency, which happened parallel with the neuronal membrane potential change. The frequency increase was more robust than in the astrocytes surrounding depolarizing neurons (maximal frequency: 1.5 ± 0.14/min; n = 5) and did not show decay. **i-j.** Astrocytes around neurons that did not respond to ACEA showed a relatively high initial calcium wave frequency (1.22 ± 0.08/min) that did not change significantly (1.16 ± 0.1/min; n = 4) during the application of the drug. Additional dashed lines on the lower trace indicate the averages of astrocytic calcium wave frequencies around neurons responding with depolarization (a; value from panel f) or hyperpolarization (b; value from panel h).

Fig. 4. CB1 receptors located on astrocytes are responsible for neuronal membrane potential changes in response to ACEA. **a-c.** Micrographs of a 1-µm-thick confocal optical section illustrating the co-localization between astrocyte specific GFAP immunostaining (a) and CB1 receptor immunolabeling for (b). Double labeled profiles on the superimposed image (c) are marked with arrowheads. On average, 21.28 ± 1.91 % of CB1 receptor positive puncta were co-localized with GFAP-immunopositivity (624 dots from 3 animals). Scale bar: 5 µm. **d.** Calcium level changes in three OGB-loaded astrocytes. The CB1 receptor agonist ACEA (5 µM) did not change the frequency of astrocytic calcium waves in CB1 receptor knockout mice. **e.** The presence of

tetrodotoxin in the bath did not prevent astrocytic calcium wave frequency increase upon ACEA application. **f.** Preincubation of thapsigargin diminishes basal astrocytic calcium waves, prevents their frequency increase during ACEA application and **(g)** significantly reduced neuronal membrane potential changes ($p = 0.0066$; n = 7; resting membrane potential, ΔRMP; firing frequency, ΔFreq; control conditions, grey dots; thapsigargin preincubation, black dot). **h.** Changes of astrocytic calcium wave frequency under control conditions (hollow bars) and during application of ACEA (black bars). Considering all loaded astrocytes, in wild type animals ACEA elicited an increase of calcium wave frequency (from 0.57 ± 0.07/min to 0.91 ± 0.09/min; $p = 0.001$). In CB1 knockout mice, the control calcium wave frequency was significantly lower than in the wild type (0.24 ± 0.09/min; $p = 0.0064$, n = 73), and frequency increase to ACEA is not significant (0.27 ± 0.08/min; $p = 0.39$). In the presence of TTX, in wild type animals the calcium wave frequency under control conditions was low (0.09 ± 0.03/min; $p = 0.0004$ compared to the control in n aCSF; n = 53) and ACEA evoked a large, significant frequency increase (0.56 ± 0.12/min; $p = 0.0001$). Thapsigargin diminishes all calcium waves (n = 58).

Fig. 5. Increased endocannabinoid tone prevents membrane potential changes in certain neurons. **a.** The original firing frequency of the neurons (n = 46) is inversely proportional to the ACEA evoked membrane potential change ($S = -0.8046$, $p = 0.019$). **b.** Astrocytic calcium wave frequency change also shows an inverse relationship with the original frequency of astrocytic calcium waves ($S = -0.8545$, $p = 0.0015$). **c.** Membrane

potential registration of a neuron (upper trace) and calcium waves in the neighboring astrocytes (three lower traces) in a slice preincubated with low concentration of ACEA (50 nM). Horizontal bars above the voltage trace represent the periods of application of ACEA in different concentrations. Note the high basal firing frequency of the neuron and the high basal frequency of astrocytic calcium waves. **d.** Time course of the neuronal membrane potential (top) and astroglial calcium wave frequency (bottom) changes. Each data point represents the average of 30 seconds. The calcium wave frequency of astrocytes preincubated with 50 nM ACEA was significantly higher (0.62 ± 0.08/min; $p = 0.0001$; $n = 120$) than the basal calcium wave frequency of astrocytes in the vicinity of neurons that depolarized (b) or hyperpolarized (c) to ACEA, but significantly smaller than the average calcium wave frequency of astrocytes next to neurons not responding to ACEA (a) ($n = 48$, $p = 0.0001$). Application of 5 µM ACEA did not elicit a significant further change of the calcium wave frequency (0.66 ± 0.1/min). The dashed lines indicate the averages of the calcium wave frequency of astrocytes. The dashed line without a label belongs to astrocytes in slices preincubated with 50 nM ACEA. **e.** Neuronal membrane potential (ΔRMP) and firing frequency (ΔFreq.) changes in response to 5 µM ACEA without preincubation (grey dots) and after preincubation with 50 nM ACEA (black dots). Preincubation with a low dose of ACEA significantly reduced but did not diminish neuronal responses ($p = 0.021$ compared to the changes obtained without preincubation with low dose of ACEA; $n = 15$).

Fig. 6. Suprathreshold neuronal depolarization elicits calcium waves on the neighboring astrocytes in a CB1 receptor dependent way. **a.** Patched neuron (asterisk) and OGB

loaded astrocytes in a PPN slice prepared from a wild type mouse. **b.** Action potential discharge (top trace) during a 10 mV depolarization of the neuron (with asterisk on panel A) evoked by current injection and the average of intracellular calcium concentration changes produced by 7 neighboring astrocytes (bottom trace). Vertical dashed lines indicate the period of the current pulse. **c.** Time course of astrocytic calcium wave frequency changes. Each data point represents the average of 30 seconds. The frequency increased significantly during neuronal depolarization ($p = 0.004$). **d-f.** The same depolarization in a neuron from a CB1 knockout animal could only evoke mild calcium wave frequency increase in neighboring astrocytes ($p = 0.058$).

Fig. 7. Proposed model of endocannabinoid signaling in the PPN. 1. Active PPN neurons synthesize endocannabinoids (ECB). 2. Endocannabinoids activate CB1 receptors on astrocytes. 3. Astrocytes, in turn, increase their calcium wave frequency and release gliotransmitters such as glutamate. Glutamate either acts on neighboring neurons via activation of group I metabotropic glutamate receptors and hyperpolarizes them (4a), or depolarizes neurons through group II mGluRs (4b.) Glutamate might activate astrocytic glutamate receptors as well (hollow green arrows). These astrocytic mGluRs can possibly lead to modifications of gliotransmitter release, thus contributing to the observed effect (indicated by the red arrows and question marks; for details see Discussion).

Figure 7.
Click here to download high resolution image

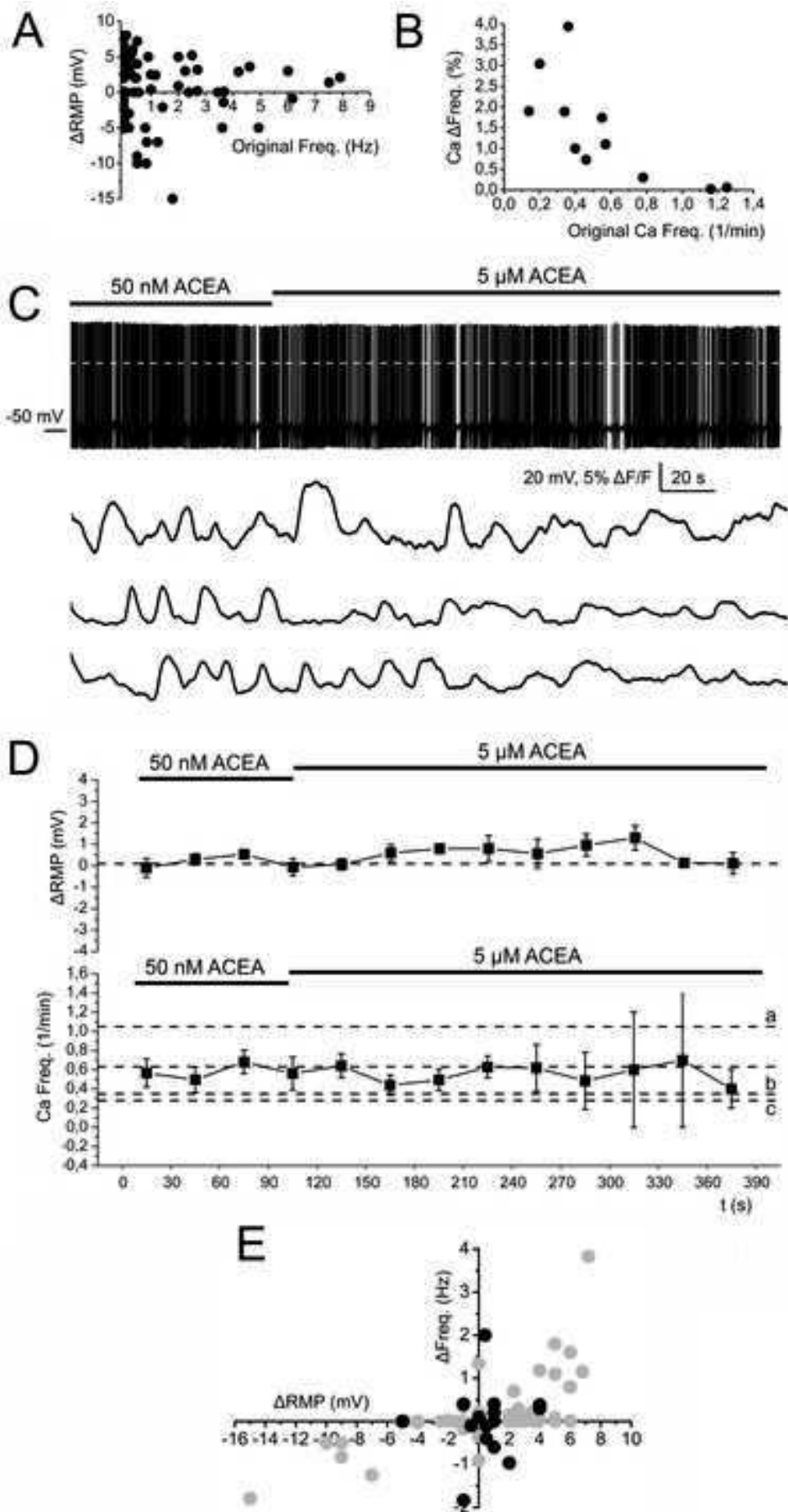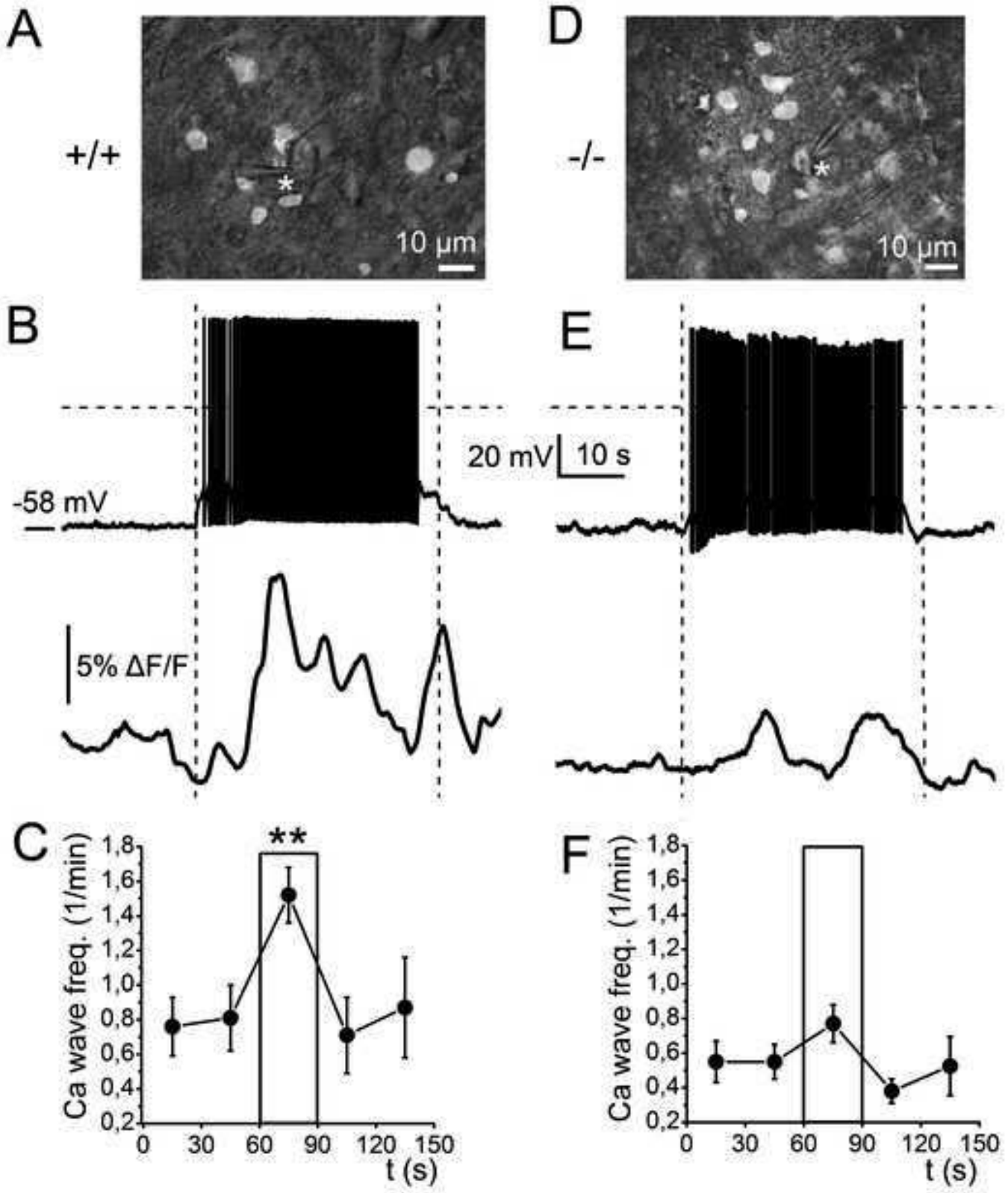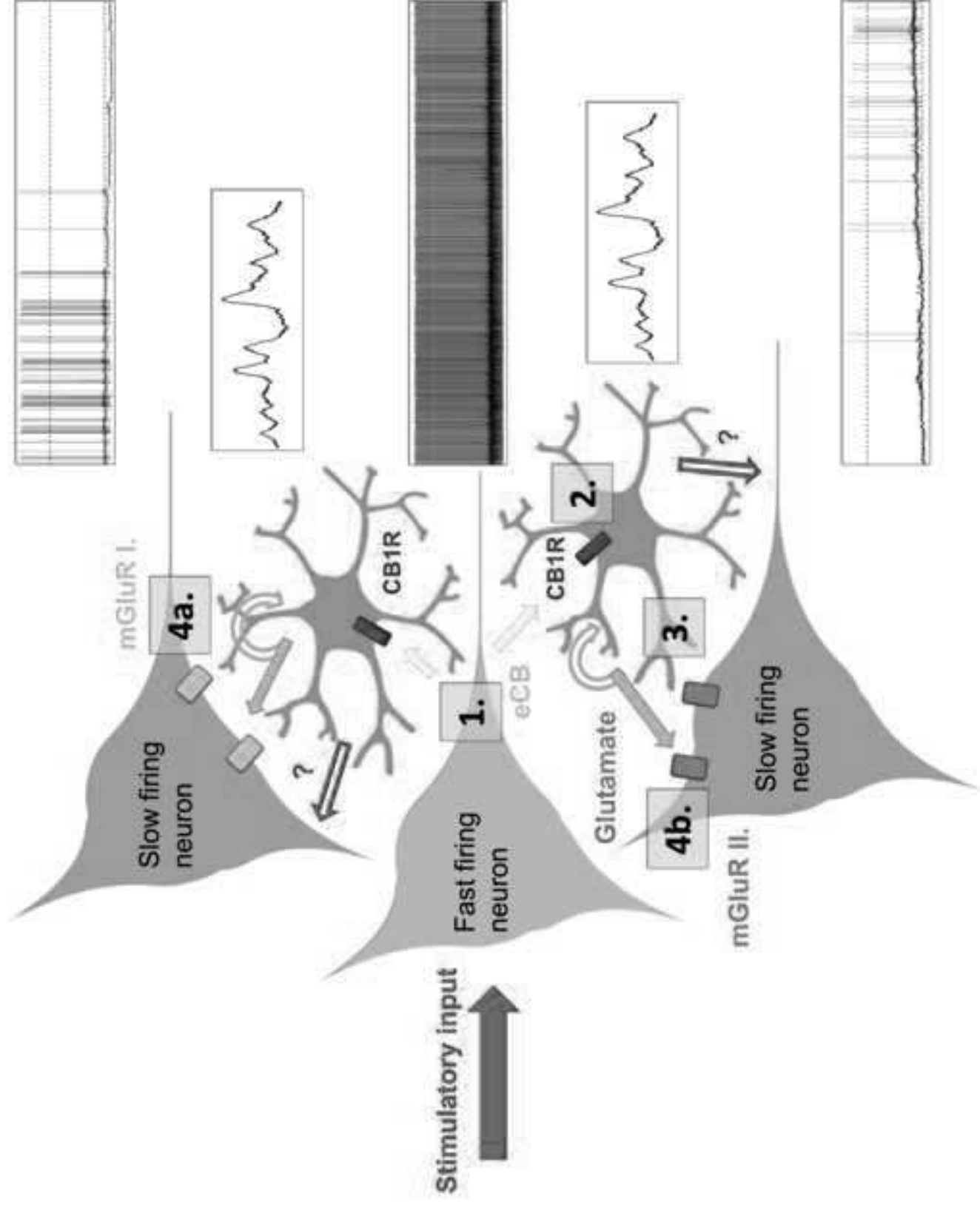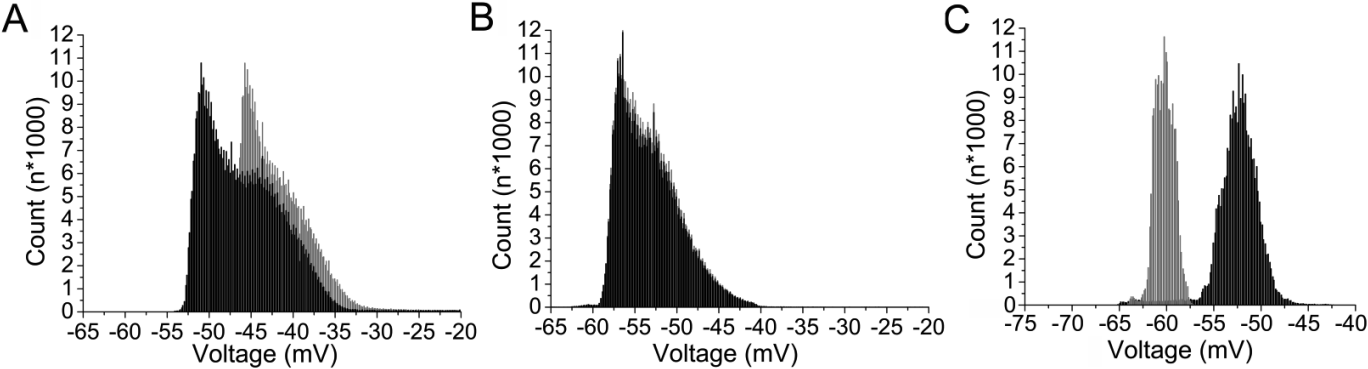**Suppl. Fig. 1.** Representative membrane potential histograms of 120-second-long traces from neurons responding to the CB1 receptor agonist ACEA in different ways (black columns = control, red columns = application of ACEA). a. Membrane potential histogram of a neuron depolarized by ACEA. b. Membrane potential histogram of a neuron lacking response to ACEA. c. Membrane potential histogram of a neuron hyperpolarized by ACEA.
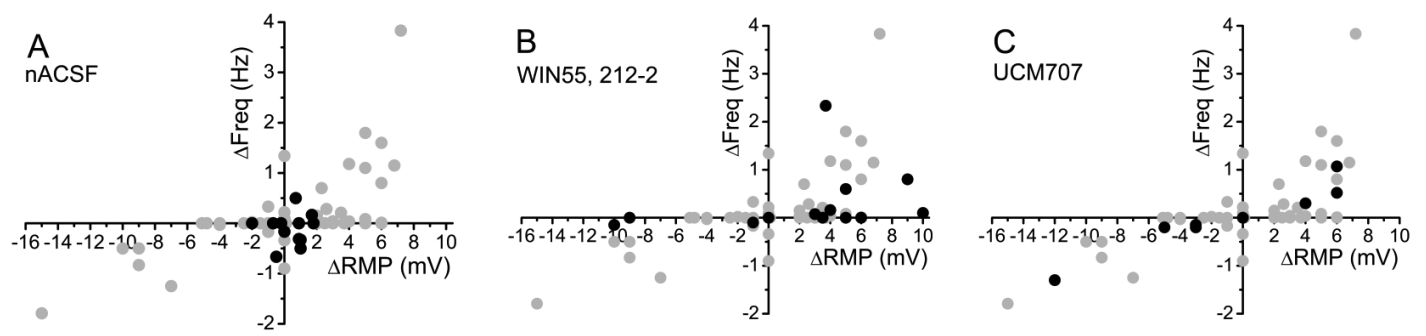
Suppl. Fig. 2. a. Spontaneous fluctuations of the membrane potential and firing rate (black dots) and changes of the same parameters upon application of 5μM ACEA (gray dots; the same in panels b-c) **b.** The effect of WIN55,212-2 (1 μM) on PPN neurons (black dots) **c.** Membrane potential and firing rate changes after application of anadamide membrane transport inhibitor UCM707 (10 μM). Membrane potential change is indicated on the X axis while firing frequency change appears on the Y axis.